

Improving Electrochemical Properties of [TiC (N) / TiNb (CN)]_n Multilayer Films Obtained on 316L Stainless Steel for Biomedical Applications

W. Aperador*, A. Delgado, M. Plaza

Facultad de Ingeniería. Universidad Militar Nueva Granada, Carrera 11 No. 101-80, Fax:+57(1) 6343200, Bogotá, Colombia.

*E-mail: g.ing.materiales@gmail.com

Received: 29 January 2014 / Accepted: 8 March 2014 / Published: 23 March 2014

In this work, a [TiC (N) / TiNb (CN)]_n multilayer film was deposited using a multi-target magnetron sputtering system, on 316 LVM steel substrates, in order to reduce wear and the release of metal ions, problems associated with steel biocompatible. Electrochemical evaluation of the multilayer is carried out by means of electrochemical impedance spectroscopy using Hank's solution as electrolyte; the tests were performed in function of time at 0, 48, and 720 hours at a temperature of 37 ° C. The morphological characterization of the mechanism of attack on the surfaces after the test was performed by scanning electron microscopy. The corrosion products were determined by X-ray diffraction, it was determined that the multilayer-coated steel systems [TiC (N) / TiNb (CN)]_n reached all-time improvements assessed. Which is attributed to an increase in the density and in the number of interfaces of the multilayer coatings, which causes the energy required for the Cl⁻ions traverse these is greater interfaces, therefore, the amount of ions is reduced to attack the substrate.

Keywords: biocompatible, corrosion, multilayer coatings.

1. INTRODUCTION

The 316 LVM stainless steel is widely used as permanent implant; however it has been demonstrated than when coming into service releases metal ions Fe, Cr and Ni, which migrated into the surrounding tissues, this causes DNA damage, alterations associated with the etiology of cancer, increases the risk of local tumors and the mechanical failure of the bioimplant [1]. The nickel content in the AISI 316 LVM is the main inconvenient [2]. Toxicological and biological test put in evidence that nickel ions in the tissue cause genotoxicity and mutagenic activity. The resistance that offers the AISI 316 LVM to corrosion in presence of biological fluids is high. Nevertheless, the passivation layer

that is formed, it is highly susceptible to pitting corrosion, one of the localized attack phenomena typical for stainless steels, which limits its use in bio-systems. The pitting corrosion affects directly the bio-compatibility and the mechanical behavior of the implant [3].

An essential characteristic of a biomaterial is that it has to be inert in the workplace, however, is unusual it happen. The human body, for being an aqueous medium, promotes the corrosive phenomena development in the metallic implants, which are denominated electrochemical processes. The biocorrosion has been one of the problems that face the durability of implants in the human body. The corporal fluids are highly hostile to metals, whereby the use of metallic alloys as biomaterials is limited by the aggressiveness of the physiological medium [4-5].

The corrosion resistance of the bio-alloys is due to the presence of an oxide layer on the surface which is of passivating character [6]. The physical-chemical property of such layer determinates the performance facing the corrosion, the interaction with the surrounding tissue of the replaced part into the body and the biocompatibility grade [7].

The passive layer that forms on the stainless steel contains two regions; one inert zone mainly formed by chrome oxide (Cr_2O_3), the other region is conformed by an iron and nickel oxides mix [6]. The resistance of the passive layer in the stainless steels is relatively high, nevertheless, is highly susceptible to pitting corrosion, which is one of the most severe localized corrosion types that attacks the stainless steel and limit its use in biomedical applications. Variety of superficial treatments and/or coatings, are made in biomaterials with the purpose of increase the corrosion resistance, the wear and the biocompatibility [8-9]. The performance of the implant through the superficial film/tissue relation and the possible transfer of metal ions from base metal to nearby tissue are vital [10-12].

Hard coatings such as the nitrides based on transition metals deposited by techniques as the physical vapor deposition and on diverse steel substrates, have been used to improve the biocompatibility substantially as is the case of the TiN with the purpose of use them as strategy to avoid the passing of metallic ions into the organism and reduce the wear in hip replacements mainly [8-9].

In this work was made a study of the electrochemical behavior of the 316 LVM steel coated with multilayers of $[\text{TiCN}/\text{TiNbCN}]_n$ with periods of 1, 50 and 150 bilayers, using as a simulated biologic fluid Hank's solution. It was determined the characteristics of the superficial layer generated in a physiological medium, with the purpose to control the potential toxicity of the metallic ion releasing in the organism.

2. EXPERIMENTAL DEVELOPMENT

2.1. Obtaining of the coating

The multilayers of $[\text{TiCN}/\text{TiNbCN}]_n$ were deposited on 316 LVM steel substrates for measurements of degradation properties in contact with simulated fluids. The coatings were obtained by a hybrid technique of sputtering called reactive magnetron sputtering r.f. (PVD) assisted with polarization voltage negative r.f applied to different substrates. Two targets were used: stoichiometric

titanium carbide, TiC, and niobium, Nb, both with 4 inches (~ 10cm) in diameter and ~ 5 mm of thickness, with purity of 99.99%. All the substrates are subjected to a cleaning process of its surface of organic contaminants beginning with an ultrasonic system, immersed in an ethanol and acetone sequence during 15 minutes per cycle. Before of the deposition, the vacuum chamber is evacuated by mechanical and turbomolecular pumps until a base pressure of 7.2×10^{-5} mbar with the aim of reduce the residual air effects.

Inside the chamber, the substrates are subjected during 15 minutes to a bias voltaje of -400 V (r.f.) with a power of 60 W (r.f.) in the argon (Ar) plasma to remove of the surface other contaminating impurities. The cathodic pulverization equipment has a positioning system of the substrate in relation to the target, this parameter allows to change the number of bilayer (n) that go from 1, 50 and 150; modifying the bilayer period (Λ). The total thickness of the deposited [TiCN/TiNbCN]_n multilayers were 3 μm approximately for all the coatings. The individual thickness varied in function of the bilayers number n=1 to n=150 produced layers with a period of 15nm at 1.5 μm respectively.

2.2 Evaluation techniques

For the corrosion resistance evaluation in static conditions was performed a potentiostat-galvanostat, Gamry PCI-4 model. The electrochemical impedance spectroscopy technique (EIS) was used. The electrochemical corrosion tests were performed at a temperature of 37 ± 0.2 °C, using as electrolyte Hank's solution (Hanks balanced salt solution, Sigma) whose chemical composition is detailed in the table 1, the tests were performed in function of time at 0, 48 and 720 hours.

Table 1. Chemical composition of the electrolyte (Hank's solution).

Compound	Concentración (g/l)
NaCl	8
D-Glucosa	1
MgSO ₂ 7H ₂ O	0.7
Na ₂ HPO ₄	0.48
KCl	0.4
NaHCO ₃	0.35
CaCl ₂ .H ₂ O	0.18
MgO ₂ .6H ₂ O	0.08
KH ₂ PO ₄	0.06

For mounting was employed a cell composed of a counter-electrode of platinum, a reference electrode of Ag/AgCl and as working electrode was used the 316 LVM steels with and without coating of [TiCN/TiNbCN]_n with an exposed area of 1 cm². The Nyquist diagrams were obtained making frequency sweeps in a range of 0.001 Hz to 100 kHz, using a sinusoidal signal amplitude of 10 mV. The superficial characteristics were determinate with SEM Phenom FEI equipped with an optical light with a magnification range of 525-24,000X. The SEM technique allows the microstructural study at

the 0 hours of exposition and later at the 192 hours of evaluation. The identification of the generated corrosion products on the steels surface was made by X-Ray diffraction (RXD). The experimental arrangement in X-ray diffraction correspond to a PW3050/60 (θ/θ) goniometer, managing under a XPERT-PRO system using a monochromatic radiation of Cu-K α 1.54 Å, operated at 40 kV and 40 mA under the temperature conditions of 25 ° C. The scanning on the surface was performed from $2\theta = 20.01^\circ$ and $2\theta = 99.99^\circ$ with a pass of $2\theta = 0.02^\circ$ at 1 second of scanning time.

3. RESULTS AND DISCUSSION

In the figures 1 is observed the Nyquist diagram for the AISI 316 LVM steel with and without coating with [TiCN/TiNbCN] $_n$ multilayers.

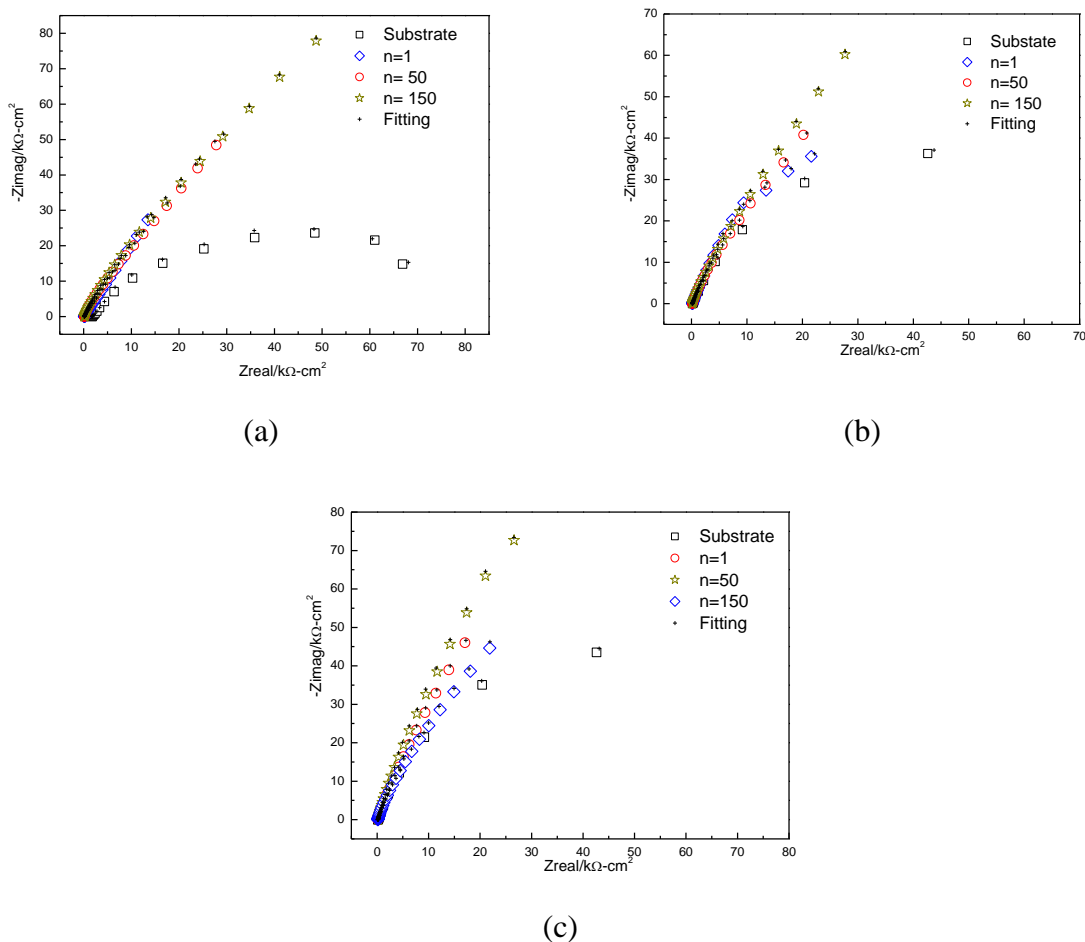


Figure 1. Nyquist diagram generated for the 316 LVM coated with [TiCN/TiNbCN] $_n$ multilayers and exposed in an electrolyte Hank’s solution evaluated at a) 0, b) 48 and c) 720 hours

It shows how the corrosion resistance (R_{cor}) changes in function of the immersion time for the different multilayers. Within the first 48 hours, the resistance has a fall that can be attributed to the

corrosion generated by the coating porosity. After the 48 hours of immersion for the films whose periods are 1, 50 and 150, the multilayers present a slightly increase in the R_{cor} possibly attributed to the corrosion products have stoppered the pores increasing the resistive way [13-15].

With reference to the multilayers and the immersion time, It is observed that this parameter takes higher values in the multilayers than in the AISI 316 LVM steel indicating that these coatings offers a better protection against the corrosion. In relation with the change that experiments the R_{pol} through the time is appreciated that for the most of the multilayers in the first hour of immersion the polarization resistance presents a high value, however, at 48 hours is appreciated a decrease of R_{pol} , finally stays constant up to 720 hours.

With the purpose of find a relation between the porosity and the different coatings, it was calculated a porosity factor associated to the different multilayer system according to W. Tato and colleagues [16], the porosity factor (porosity percentage of the layer) correspond to the relation among the polarization resistance of the substrate without coating and the coated substrate with multilayers as is shown in the following equation:

$$P = \frac{R_{p,u}}{R_{p,r-u}}$$

Where P is the layer porosity or total coating, $R_{p,u}$ is the polarization resistance of the substrate without coating and $R_{p,r-u}$ is the polarization resistance measure from the substrate-layer (Table 2). In the figure 2 is presented the porosity factor of the obtained values for the $[TiCN/TiNbCN]_n$ multilayers, which were obtained substituting the electrochemical results in the equation (1), for all the layers. In the figure 2 is present the porosity of the layer in function of the bilayers number, so that the analysis of the porosity factor applied in all layers suggests that the porosity decrease with the increase of the bilayers number (n), interfaces number and reduction of the period (Λ), additionally the behavior described above is observed where the protector factor of the multilayers is reduced at the 48 hours and stabilized at prolonged time as it was obtained at 720 hours [17-18].

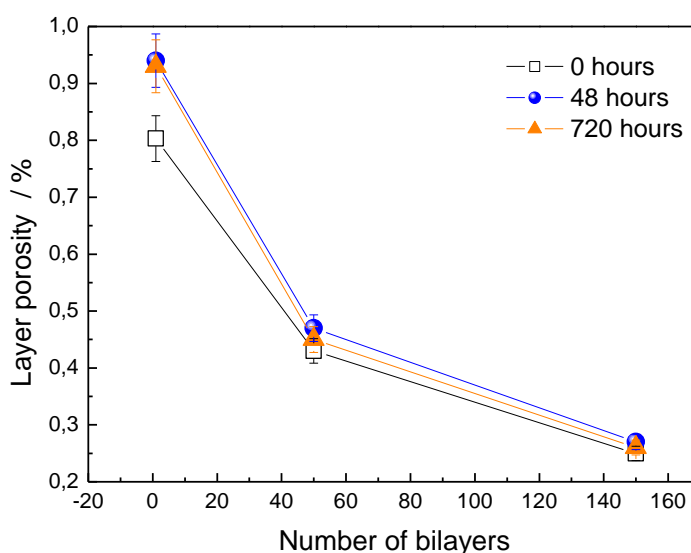


Figure 2. Porosity factor of the layer in function of the bilayers number in the multilayers of $[TiCN/TiNbCN]_n$.

The Nyquist diagrams content also simulated data. The figure 3 shows the equivalent electric circuit used in the simulation of the impedance data. The table 2 includes the used parameters in the simulation. The values of such parameters have been obtained using a non linear program of complex least squares (CNLS). As can be observed in the figures 1a, 1b and 1c is an excellent concordance between experimental and simulated data. The Nyquist diagrams have been simulated by the equivalent circuit of the figure 3a, for the substrate and 3b for the multilayers.

Table 2. Used parameters in the simulation data of the steel with and without coating evaluated at 0, 48 and 720 hours.

	R_{Ω} $\Omega \text{ cm}^2$	CPE_1 $\mu\text{F cm}^{-2}$	α_1	R_1 $10^3\Omega \text{ cm}^2$	CPE_2 $\mu\text{F cm}^{-2}$	α_2	R_2 $10^3\Omega \text{ cm}^2$
				0 hours			
n=1	61.2 (0.5%)	6.21 (3%)	0.79 (0.2%)	15.64 (4%)	65.39 (3%)	0.94 (0.6%)	96.23 (2%)
n=50	63.3 (0.5%)	11.23 (1 %)	0.74 (0.3%)	21.12(4%)	153.32 (2%)	0.93(0.8%)	196.4 5(3%)
n=15	62.4 (0.8%)	12.37 (0.5%)	0.72 (0.6%)	45.23(2%)	213.21(1%)	0.92 (0.4%)	339.11 (2%)
0							
Subst rate	63.37 (0.9%)	152.24(0.5%)	0.94(0.8%)	86.24(1%)			
48 hours							
n=1	59.7 (0.6%)	5.54 (2%)	0.82 (0.3%)	12.34 (4%)	54.54 (3%)	0.89 (0.4%)	84.23 (3%)
n=50	56.3 (0.6%)	9.82 (0.9%)	0.73 (0.5%)	15.23(3%)	140.80 (2%)	0.85 (0.5%)	165.34 (2%)
n=15	68.3 (0.4%)	10.54 (1.2%)	0.78 (0.2%)	36.58(3%)	197.12(3%)	0.91 (0.3%)	290.45 (7%)
0							
Subst rate	64.5 (0.4%)	127.31 (1.4%)	0.91 (0.6%)	79.81(2%)			
				720 hours			
n=1	66.2 (0.3%)	5.68 (3%)	0.88 (0.5%)	13.12 (3%)	59.33 (4%)	0.89 (0.7%)	89.27 (3%)
n=50	64.2 (0.4%)	10.74 (0.4%)	0.79 (0.4%)	19.21(3%)	46.21 (4%)	0.82 (0.3%)	181.86 (6%)
n=15	63.7 (0.8%)	11.39 (0.8%)	0.89 (0.3%)	42.21(2%)	206.32 (2%)	0.93 (0.5%)	316.14 (3%)
0							
Subst rate	62.3 (0.3%)	136.15(0.9%)	0.92 (0.5%)	83.22(3%)			

In all Nyquist diagrams of the figures 1 is observed a capacitive behavior at high frequencies, defining a semicircle flattened in which the center is located below the real axis. This flattening phenomenon of the semicircle is associated with a dispersion process in the frequency, due to electrode

surface is not homogeneous. The figure 3a shows the impedance of the electrodes that consists in the solution resistance R_s , in series with the connection in parallel of the double layer capacitance and the faradic impedance, corresponding to Randles diagram.

The proposed equivalent circuit to model the multilayers behavior has been schematized in the figure 3b, this model considers the wear of the films deposited by PVD generally is located in the permeable pores, where the corrosive electrolyte penetrates into the substrate, therefore the ceramic coating can be consider as a leaky capacitor. The equivalent circuit contents two constant phase elements distributed inside the circuit (CPE1 and CPE2) which allows considering the two relaxation time constants. It was obtained that the couple of CPE1-R1 predominates in high frequencies and may be due to the passive layer and/or the dielectric properties of the multilayers, while the (CPE2-R2) couple at low frequencies shows a characteristic of the protection process between steel/multilayers which is associated to the pores diminution, that is presented at increase the quantity of bilayers [19].

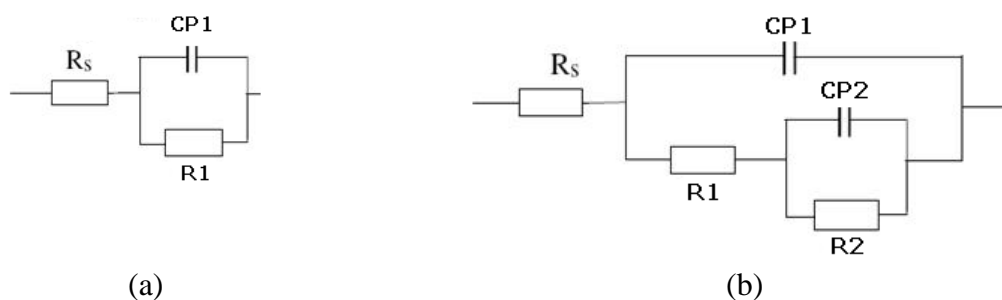


Figure 3. Equivalent circuit used to model the impedance behavior a) substrate b) coatings evaluated at 0, 48 and 720 hours.

SEM

The superficial analysis of the coatings in the multilayer system was performed by scanning electron microscopy (SEM) immediately after the electrochemical tests end. The figure 4 shows microscopies of the surface on the multilayers, all the images were taken in the same conditions of magnification and illumination, with the purpose to observe the degradation phenomena in relation to the bilayers number and the interfaces [20].

In the Figures 4a, b and c is clearly show the superficial degradation, due to the chemical attack by the Hank's solution. In the different $[\text{TiCN}/\text{TiNbCN}]_n$ multilayers, the degradation level was proved to be dependent on period of bilayer, making more evident the chemical attack in the multilayers with lower bilayer period. The degradation grade is the same for the coatings in the evaluation of the 48 and 720 hours. However, is only reported the coating with highest exposure time [21].

From the above we can emphasize, that there is an important contribution of the interfaces within the multilayer system to reduce from chemical attack, presumably due to the ions of the Hank's solution change the direction each whenever is found a new interface allowing in this way that the electrochemical potential increases, which promotes the corrosion resistance, also the increase of the interfaces promotes likely the porosity reduction in the multilayers.

The effect of porosity reduction is more significant in the electrochemical systems with a high number of bilayers or a great number of interfaces evidencing low corrosion velocities in comparison with the deposited layers with lower number of bilayers.

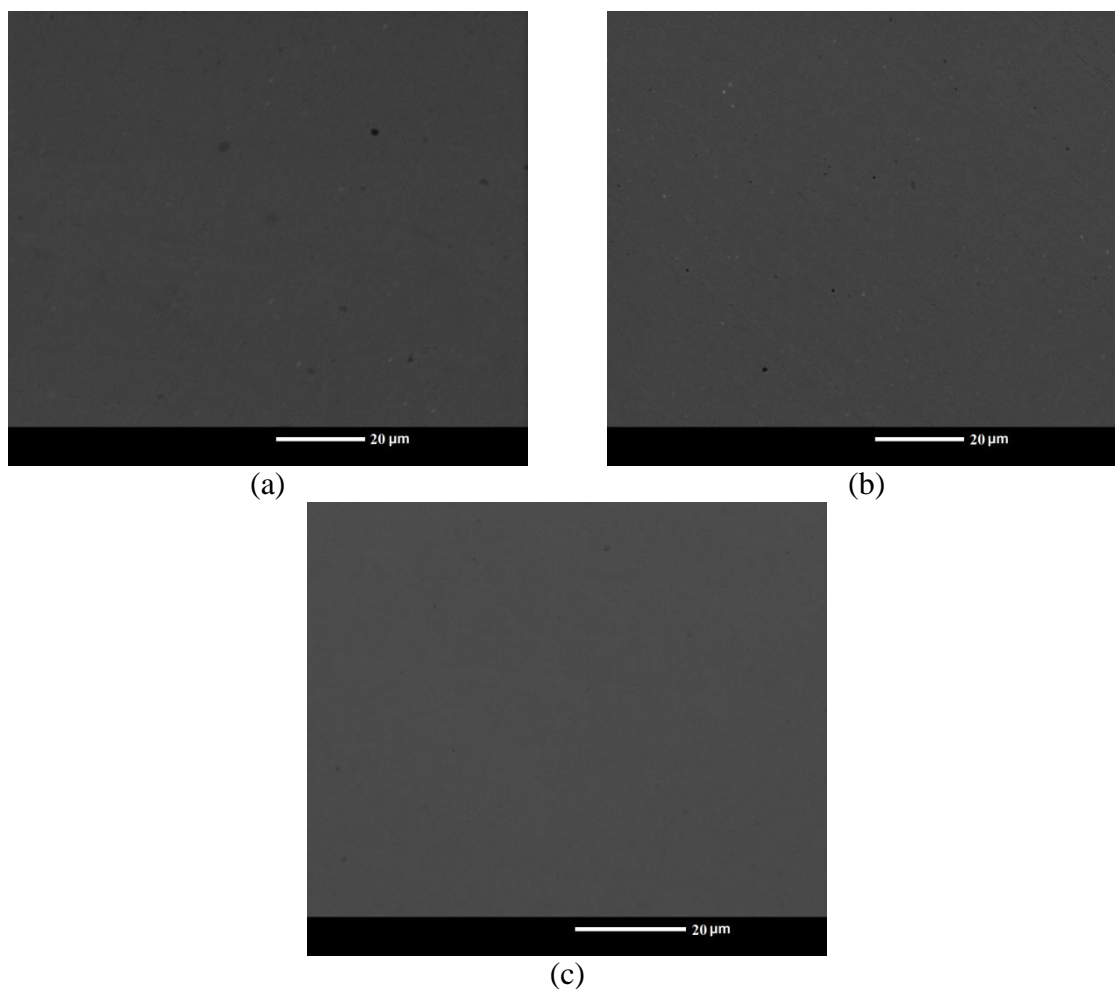


Figure 4. SEM micrographs for samples evaluated at the Hank's solution for 720 hours (a) bilayers with $n = 1$ b) $n = 50$, c) $n = 150$.

XRD

In the figure 5 is observed the crystalline planes (111) (200) (222) of the TiNbCN, and TiCN (200) (220) corresponding to a FCC structure. Furthermore, it can be appreciated that the intensity peaks of the (111) plane are increasing as the period of the multilayers increases suggesting that be the preferential. The preferred orientation of the (111) is related to the multilayer grow in those planes where the superficial energy and deformation are minimum, this indicates that for the multilayers with $n=150$ has minimum values of the mentioned energy increasing and converting in the preferred plane. Also appears in the figure 4 the corresponding peaks of the TiCN that remain for large bilayer periods as well as small. The presence of such peak is due to the interlayer of Ti combined with the C and N deposited to improve the adhesion of the multilayer. In any of the multilayers is observed corrosion

products of the AISI 316 LVM steel, indicating the good performance that is reached with this kind of coating.

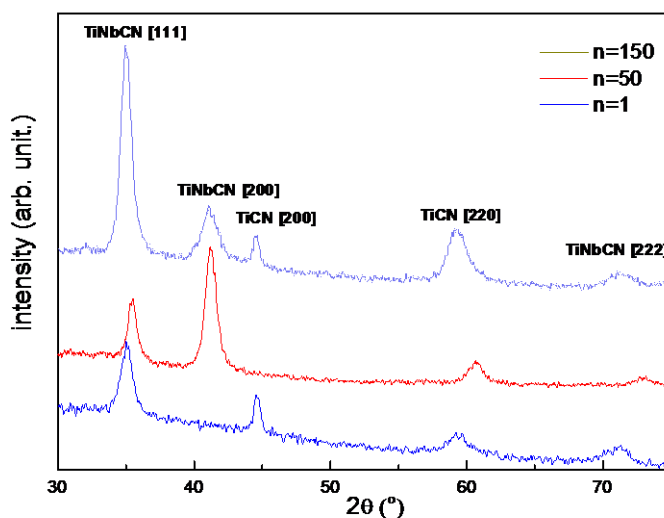


Figure 5. X-ray diffractogram of the films TiNbCN different number of bilayers and evaluated after the corrosion wear test.

4. CONCLUSIONS

The [TiCN/TiNbCN] n multilayers deposited on AISI 316 LVM steel indicate that these coatings offer better protection against corrosion, due to its corrosion resistance was high in all the multilayers. The established parameters in the bilayers allow to indicate that the corrosion resistance at the first hours of evaluation presents a high value. Subsequently to 720 hours, these parameters indicate a stabilization that allows to determine its adequate corrosion resistance and biocompatibility, which makes suitable to be used as biomaterial. By SEM and XRD was characterized the metallic surface after the immersion test in the artificial solution. Obtaining a surface with stability and high corrosion resistance as well as a high relation of bilayers number.

ACKNOWLEDGEMENTS

This research was supported by Vicerrectoría de Investigaciones Universidad Militar Nueva Granada.

References

1. R. Altobelli, M. C. Lopes de Oliveira, *Acta Biomaterialia*, 8 (2012) 937.
2. D.J. Wever, A.G. Veldhuizen, M.M. Sanders, J.M. Schakenraad, J.R. van Horn, *Biomaterials*, 18(1997) 1115.
3. M. Lundin, Y. Hedberg, T. Jiang, G. Herting, X. Wang, E. Thormann, E. Blomberg, I. Odnevall Wallinder, *Journal of Colloid and Interface Science*, 366 (2012) 155.
4. Z. Yang, J. Wang, R. Luo, M. Maitz, F. Jing, H. Sun, N. Huang, *Biomaterials*, 31 (2010) 2072.
5. Z. Bai, M.J. Filiaggi, J.R. Dahn, *Surface Science*, 603 (2009) 839.

6. A.M. Gallardo-Moreno, M. Multigner, A. Calzado-Martín, A. Méndez-Vilas, L. Saldaña, J.C. Galván, M.A. Pacha-Olivenza, J. Perera-Núñez, J.L. González-Carrasco, I. Braceras, N. Vilaboa, M.L. González-Martín, *Materials Science and Engineering: C*, 31 (2011)1567.
7. S. Karimi, T. Nickchi, A. M. Alfantazi, *Applied Surface Science*, 258 (2012) 6087.
8. C. Liu, G. Lin, D. Yang, M. Qi, *Surface and Coatings Technology*, 200(2006) 4011.
9. L. Chenglong, Y. Dazhi, L. Guoqiang, Q. Min, *Materials Letters*, 59 (2005) 3813.
10. K. M. Kruszewski, L. Nistico, M. J. Longwell, M. J. Hynes, J. A. Maurer, L. Hall-Stoodley, E. S. Gawalt, *Materials Science and Engineering: C*, 33 (2013) 2059.
11. D. Chicot, E.S. Puchi-Cabrera, X. Decoopman, F. Roudet, J. Lesage, M.H. Staia, *Diamond and Related Materials*, 20 (2011) 1344.
12. A. Thaveedetrakul, N. Witit-anun, V. Boonamnuayvitaya, *Applied Surface Science*, 258 (2012) 2612.
13. R.A. Antunes, A.C.D. Rodas, N.B. Lima, O.Z. Higa, I. Costa, *Surface and Coatings Technology*, 205 (2010) 2074.
14. L. Mohan, C. Anandan, V.K. William Grips, *Applied Surface Science*, 258 (2012) 6331.
15. D.V. Shtansky, I.V. Batenina, I.A. Yadroitsev, N.S. Ryashin, Ph.V. Kiryukhantsev-Korneev, A.E. Kudryashov, A.N. Sheveyko, I.Y. Zhitnyak, N.A. Gloushankova, I.Y. Smurov, E.A. Levashov, *Surface and Coatings Technology*, 208 (2012) 14.
16. W. Tato, D. Landolt, *J. Electrochem. Soc.* 145 (1998) 4173.
17. J.C. Caicedo, C. Amaya, G. Cabrera, J. Esteve, W. Aperador, M.E. Gómez, P. Prieto, *Thin Solid Films*, 519 (2011) 6362.
18. C.-Mihai Cotrut, V. Braic, M. Balaceanu, I. Titorencu, M. Braic, A. Constantina Parau, *Thin Solid Films*, 538 (2013) 48.
19. J.C. Caicedo, C. Amaya, L. Yate, W. Aperador, G. Zambrano, M.E. Gómez, J. Alvarado-Rivera, J. Muñoz-Saldaña, P. Prieto, *Applied Surface Science*, 256 (2010) 2876.
20. J.C. Caicedo, C. Amaya, L. Yate, M.E. Gómez, G. Zambrano, J. Alvarado-Rivera, J. Muñoz-Saldaña, P. Prieto, *Applied Surface Science*, 256 (2010) 5898.
21. W. Aperador, J.C. Caicedo, R. Vera, *Int. J. Electrochem. Sci.*, 8 (2013) 2778.